This article has been accepted for publication in a future issue of this journal, but has not been fully edited. Content may change prior to final publication. Citation information: DOI 10.1109/TSTE.2018.2871074, IEEE Transactions on Sustainable Energy

PV Solar System Control as STATCOM (PV-STATCOM) for Power Oscillation Damping

Rajiv K. Varma, *Senior Member, IEEE* and Hesamaldin Maleki, *Student Member, IEEE*

***Abstract*— This paper presents a novel control of PV solar system as a FACTS device STATCOM, termed PV-STATCOM, for power oscillation damping (POD) in transmission systems. In the proposed control, as soon as power oscillations due to a system disturbance are detected, the solar farm discontinues its real power generation function very briefly (few tens of seconds) and makes its entire inverter capacity available to operate as a STATCOM for POD. As soon as power oscillations are damped, the solar farm restores real power output to its pre-disturbance level in a ramped manner, while keeping the damping function activated. This results in much faster restoration than that specified in grid codes. During nighttime, the solar farm performs POD with its entire inverter capacity. It is shown from EMTDC/PSCAD simulations that the proposed control provides significant increase in power transfer capacity on a 24/7 basis in systems which exhibit both local inertial and inter-area oscillatory modes. The proposed PV-STATCOM is about 50-100 times cheaper than an equivalent STATCOM for providing POD at the same location. This novel control can potentially bring large savings for transmission utilities and open up a new revenue making opportunity for solar farms for providing POD.**

***Index Terms*--Photovoltaic solar power systems, voltage control, reactive power control, power oscillation damping, FACTS, STATCOM, power transmission, PV ramp rate**

I. Introduction

LOW frequency electromechanical power oscillations (typically 0.1 - 2 Hz) are recognized as one of the major limiting factors in power transfer over long transmission lines [1]. Conventionally, these oscillations are damped by Power System Stabilizers (PSS) integrated with synchronous generators [1]. However, Flexible AC Transmission System (FACTS) devices have been effectively utilized in power systems for damping these power oscillations and thereby enhancing the power transfer capability in transmission lines [2-4]. Performances of various FACTS devices equipped with power oscillation damping (POD) controllers are described in literature, such as, Static Var Compensators (SVC) [5], Static Synchronous Compensators (STATCOM) [6, 7], Thyristor Controlled Series Compensators (TCSC) [8], and Convertible Static Compensator (CSC) [9].

The financial support from Ontario Centres of Excellence (OCE) and Hydro One under the grants CR-SG30-11182-11; NSERC; and Western University WSS-NSERC Accelerator program are gratefully acknowledged.

Rajiv K. Varma and H. Maleki are with the Department of Electrical and Computer Engineering, The University of Western Ontario, London, ON N6A 5B9, Canada (e-mail: rkvarma@uwo.ca; hmaleki2@uwo.ca).

Large scale PV solar farms in excess of 100 MW are being increasingly connected worldwide. These include Kamuthi (648 MW), in Tamil Nadu, India [10], Rancho Cielo Solar Farm (600 MW), Solar Star I and II (579 MW), Topaz Solar Farm (550 MW), Agua Caliente Solar Project (295 MW) California Valley Solar Ranch Farm (250 MW) in USA, and Huanghe Hydropower Golmud Solar Park in China (200 MW) [11-13]. The potential of reduction in power system stability with significant amount of inertia-less power injection from PV solar plants in the grid is described in [14-16].

Smart PV inverter controls such as Constant (off-unity) Power Factor, Volt/Var, Volt/Watt, Frequency Watt, Low/High Voltage Ride Through, Low/High Frequency Ride Through, etc., have been proposed [17] and also demonstrated on a large scale PV solar farm [18]. A novel control of PV solar farm as STATCOM (PV-STATCOM) was presented for enhancing the connectivity of wind farms in the night [19] and for increasing power transfer capacity through damping of power oscillations both during night and day [20]. This control technique utilized the entire inverter capacity in the nighttime and the inverter capacity remaining after real power generation during daytime for power oscillation damping. An eighth-order POD controller for large PV solar farm was proposed in [21], whereas an energy function based design of POD controller was presented in [22]. Both these controllers are relatively complex in design. All the POD controls in the above papers [19-22] are based on remaining inverter capacity during daytime. Hence, the proposed POD capability of solar farm is limited during day, indeed becoming zero during hours of full sun.

This paper proposes a novel PV-STATCOM control for POD, based on a patent-pending technology [23]. In this proposed control, if any disturbance occurs in the power system causing undesirable power oscillations, the PV solar farm autonomously disables its real power generating function for a short period (typically less than a minute), and makes its entire inverter capacity available for operating as STATCOM to damp power oscillations through reactive power modulation. As soon as the power oscillations are reduced to an acceptable level, the solar farm restores its power output to its pre-disturbance level in a ramped manner. Another novel contribution of this paper is that the POD function is kept activated during the ramp up of power to its pre-disturbance value utilizing the inverter capacity remaining after real power generation. This prevents any recurrence of power oscillations and also allows a much faster ramp-up than prescribed by grid codes [24] where such a damping function during ramp-up is not envisaged.

This article has been accepted for publication in a future issue of this journal, but has not been fully edited. Content may change prior to final publication. Citation information: DOI 10.1109/TSTE.2018.2871074, IEEE Transactions on Sustainable Energy

While [19] and [20] have both presented the control of PV solar farm as STATCOM, [19] has dealt with voltage control only during nighttime (not daytime) on a distribution feeder. The damping of power oscillations in transmission systems is not examined at all. Power oscillation damping control in a Single Machine Infinite Bus (SMIB) transmission system is described in [20]. This control has been demonstrated during nighttime with full inverter capacity but during daytime with only partial inverter capacity. This STATCOM control has the following limitations: i) it is available only when there is remaining inverter capacity available after real power generation, and ii) its capability declines with increasing real power output from solar farm, becoming completely zero during hours of full sun.

The novel smart PV inverter control as PV-STATCOM proposed in this paper is an altogether different control which allows power oscillation damping as follows: i) with full inverter capacity, and ii) both during night and day on a 24/7 basis.

The effectiveness of the proposed PV-STATCOM for POD is demonstrated on a Single Machine Infinite Bus (SMIB) system [25], Two-Area power system [1], and the 12 bus FACTS power system [30] through detailed electromagnetic transients studies using PSCAD/EMTDC software. The *Simplex* optimization method embedded in PSCAD/EMTDC [26] is utilized to design the POD controller.

In [27-29], the small signal Residue Analysis technique is presented for determining the most effective locations of power system stabilizer (PSS) in power systems. The same technique is utilized in this paper to investigate the effectiveness of specific PV-STATCOM locations for POD.

Section II enunciates the proposed PV-STATCOM concept. Section III describes the three study systems. The PV-STATCOM model is presented in Section IV. Section V describes the design of the POD controller. The small signal residue analysis is presented in Section VI. EMTDC/PSCAD simulation studies for the three study systems are presented in Section VII, VIII, and IX, respectively. Section X illustrates the effect of proposed PV-STATCOM control on power system frequency. The conclusions are drawn in Section XI.

II. Concept of PV-STATCOM

Fig. 1 shows the typical real power output of a PV solar farm *P* during a sunny day and the remaining reactive power capacity *Q* during a 24-hour period for that day. The proposed smart inverter PV-STATCOM has two modes of operation illustrated in Fig. 1, which are described below:

A. *Partial PV-STATCOM mode*

In this mode, the PV inverter capacity remaining after real power generation is utilized for STATCOM mode of operation. This mode is available during daytime.

B. *Full PV-STATCOM mode*

In this mode, the entire PV solar farm inverter capacity is made available for STATCOM mode of operation. During daytime, as soon as any unacceptable low-frequency power oscillations due to any system disturbance are detected, the real power generation function is discontinued. The solar inverter is then transformed into a STATCOM with the entire inverter capacity made available for reactive power modulation. Depending upon the system need, reactive power up to the entire inverter capacity can be utilized for power oscillation damping. Once the low-frequency oscillations are damped, the real power generation function is reinstated. The solar farm then ramps up its real power output to the pre-disturbance level while continuing to perform POD in the Partial PV-STATCOM mode. During nighttime, the Full-STATCOM mode is available continuously for POD with reactive power modulation utilizing the entire inverter capacity.

The solar farm has another operating mode termed Full PV mode, in which it generates real power based on available irradiance at unity power factor with no smart functions.

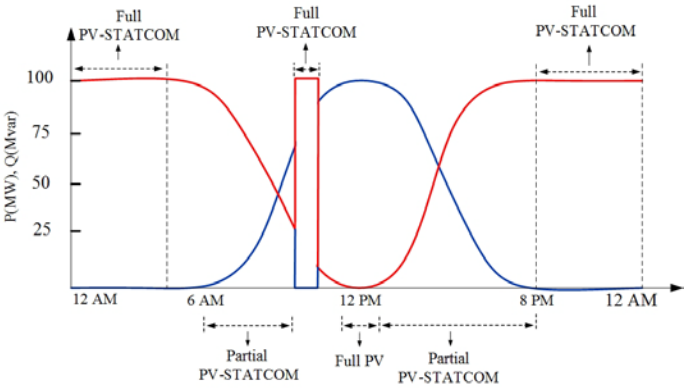

Fig. 1. PV Real and Reactive power during 24 hours on a sunny day

III. Modeling of Study Systems

A. *Study System 1: Single Machine Infinite Bus (SMIB) System*

Fig. 2 illustrates the single line diagram of the large synchronous generator connected to an infinite bus through a 600 km line [25]. A 100 MW PV solar farm connected at the mid-point of the transmission line.

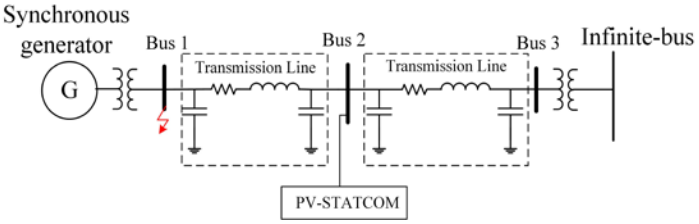

Fig. 2. Single-line diagram of an SMIB system with a 100 MW PV plant connected midline.

B. *Study System 2: Two-Area Four Machine System*

The Two-Area system having four generators connected with the 220 km tie-line [1] is depicted in Fig. 3. A 100 MW PV system is connected at the midpoint of the tie-line between buses 7 and 9. In both study systems, the synchronous generators are represented by their detailed sixth-order model and DC1-A-type exciter [1]. No Power System Stabilizer (PSS) are installed on generators. The parameters for SMIB system and the Two-Area system are provided in [1] and [25], respectively. The Two-Area system exhibits both local inertial mode and inter-area mode of oscillations in the power flow [1].

This article has been accepted for publication in a future issue of this journal, but has not been fully edited. Content may change prior to final publication. Citation information: DOI 10.1109/TSTE.2018.2871074, IEEE Transactions on Sustainable Energy

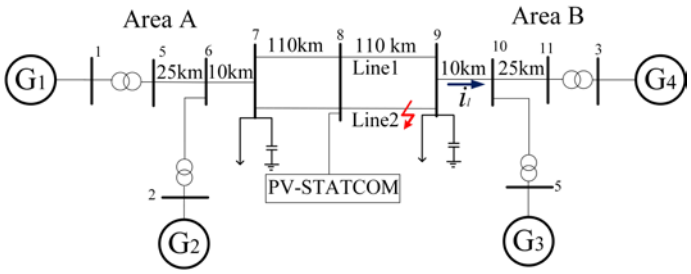

Fig. 3. Single-line diagram of Two-Area system with 100 MW PV plant connected midline.

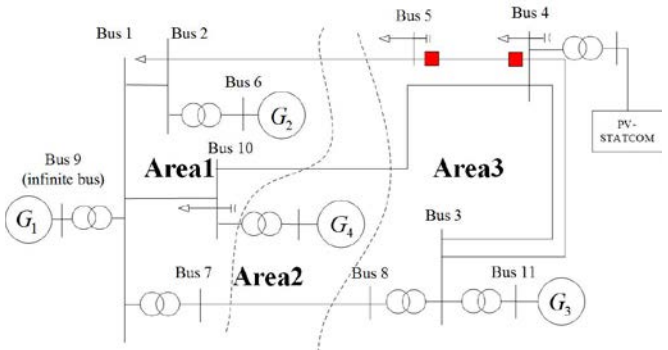

Fig. 4. 12 bus FACTS power system with 100 MW PV solar system at bus 4

C. *Study System 3: 12 Bus FACTS power system*

The 12 bus FACTS power system widely is used for studying the impact of FACTS controls [30, 31]. To demonstrate the effectiveness of the proposed controller, POD studies with PV-STATCOM are performed on the 12 bus FACTS power system having multiple oscillatory modes. In this study, no PSSs are considered on generators.

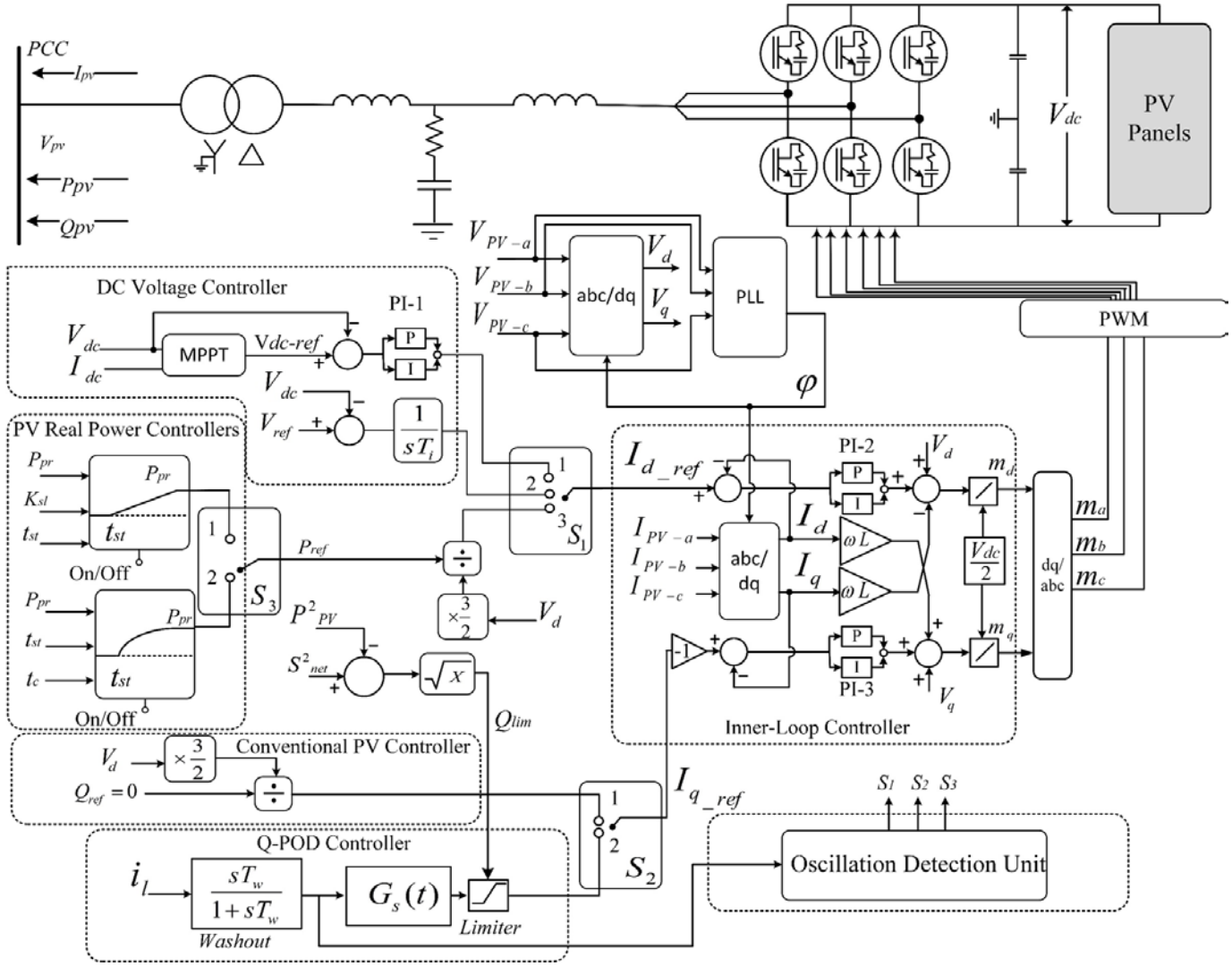

Fig. 5. PV-STATCOM controller

This article has been accepted for publication in a future issue of this journal, but has not been fully edited. Content may change prior to final publication. Citation information: DOI 10.1109/TSTE.2018.2871074, IEEE Transactions on Sustainable Energy

IV. MODELING OF PV-STATCOM

Fig. 5 portrays the different components of the PV system and the PV-STATCOM controller, which are described below.

A. *PV Panels and Inverter:*

The aggregated PV panels are represented by an equivalent panel model which generates PV dc current based on the *V-I* characteristic of the PV panels [32]. The aggregated solar farm inverter is considered to be of three-phase six-pulse configuration with a DC link capacitor [33]. The PV inverter is connected to the grid through an *LCL* filter designed based on [34]. The symbols V_{pv}, Q_{pv}, P_{pv}, I_{pv} represent the voltage, inverter reactive power, inverter real power and inverter current at the PCC, respectively.

B. *Inner Loop Controller*

The inner loop controller provides decoupled *d-q* axis control of real and reactive power based on the *d* axis reference current I_{d_ref} and *q* axis reference current $I_{q\_ref,}$ respectively [33]. This controller provides the modulation indices m_d and m_q which are transformed in the *dq/abc* block to the three phase modulation indices m_a, m_b, m_c. These are used for generating inverter triggering pulses using Pulse Width Modulation (PWM) [31]. The *abc* to *dq* transformation unit and Phase Locked Loop (PLL) unit are designed based on [33]. In Fig. 5, V_{dc} denotes the PV-STATCOM DC link voltage while V_d, I_d, V_q, I_q represent the direct and quadrature voltages and currents of PV system, respectively.

C. *DC Voltage Controller*

The DC voltage controller has two components: i) the Maximum Power Point Tracking (MPPT) block with a PI controller, and ii) a DC voltage controller [35]. During conventional PV operating mode, based on the *VI* characteristic of the PV panels, the MPPT block utilizes V_{dc} and I_{dc} to generate the reference voltage $V_{dc\text{-}ref,}$ which eventually produces I_{d_ref} for the inner-loop controller. In STATCOM control mode, S_1 changes to position 2 and the DC voltage V_{dc} is regulated to PV panel open circuit voltage to disable real power injection from the PV solar panels [36]. The open-circuit voltage is not a constant and depends on the incident irradiance and temperature. For the specifically utilized PV panel in the solar farm, the largest open circuit voltage obtained from various (manufacturer supplied) power-voltage characteristics for different realistically prevalent temperatures and solar irradiance [32] is chosen as V_{ref} for the DC link voltage controller module in Fig. 5.

D. *Conventional PV controller*

The conventional PV controller regulates the inverter reactive power such that PV power output is at unity power factor [33]. This controller has been adopted from [33], [35], [37] and is utilized only during normal operation of the power system in which unity power factor is required for PV systems. In this control, *Q* is set to zero during steady state operation resulting in I_{q_ref} = 0. It is clarified that this controller is deactivated during disturbances, i.e. during power oscillations. In this situation, I_{q_ref} is generated with the Q-POD controller in a closed loop manner

E. *Q-POD Controller*

The Q-POD controller controls the reactive power output of PV-STATCOM to damp the low-frequency electromechanical oscillations. In this paper, the magnitude of the line current at the PCC of solar farm is selected as the control signal for POD [20]. In Study System 1, i_l represents the midline current where the PV system is connected. Meanwhile, in Study System 2, i_l represents the line current between buses 9 and 10. The i_l signal is fed to the washout filter [34] to remove its steady state component. The POD controller transfer function is selected as:

$$G_s(t) = G \times \frac{1 + sT_{lead}}{1 + sT_{lag}} \quad (1)$$

where, *G* represents the controller gain; and T_{lead} and T_{lag} denote the *lead* and *lag* time constants, respectively.

The operating principle of POD controller is described in detail in [1], [5-7]. This controller effectively adds adequate phase lead or phase lag to a selected system oscillatory mode to enhance its damping. In this paper, the oscillatory modes for different study systems are selected and the corresponding optimized lead-lag controllers are designed based on an optimization process described in Section V. This POD controller generates the reference signal I_{q_ref} for PV inverter inner loop controller to control PV reactive power.

F. *Oscillation Detection Unit (ODU)*

The ODU autonomously detects the occurrence of unacceptable low-frequency electromechanical power oscillations caused by any grid disturbance such as faults.

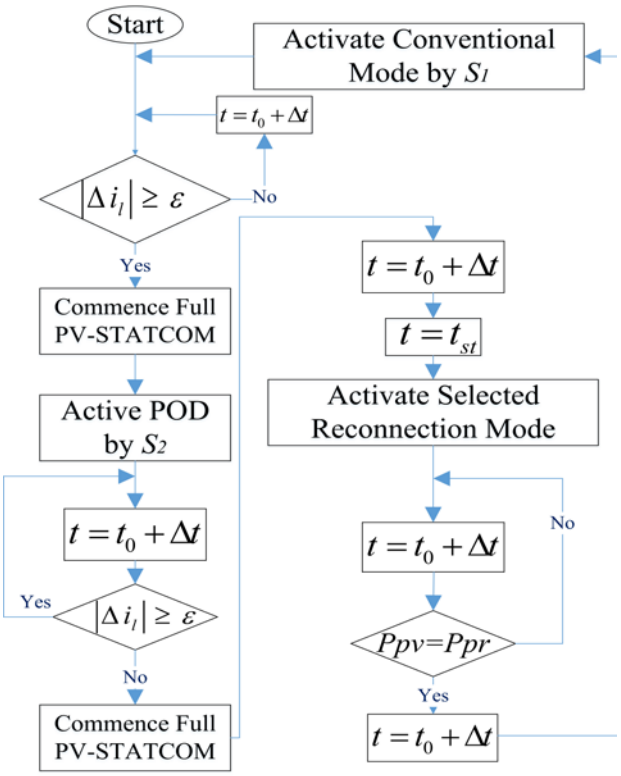

Fig. 6. Flowchart of the operation of Oscillation Detection Unit

This article has been accepted for publication in a future issue of this journal, but has not been fully edited. Content may change prior to final publication. Citation information: DOI 10.1109/TSTE.2018.2871074, IEEE Transactions on Sustainable Energy

The ODU operates based on the flow chart depicted in Fig. 6 and generates the On/Off status signals for switches S_1, S_2, and S_3. The oscillatory component of line current Δi_l is compared with a predefined value ε which in this paper is chosen as 5%. If the variation is more than ε the Full PV-STATCOM mode is activated for POD control and the PV real power is reduced to zero.

G. PV Real Power Controllers

These controllers are responsible for the restoration of real power output of the PV solar farm to its pre-disturbance level after power oscillations are damped with the Full PV-STATCOM mode of operation. Grid codes such as [39] require the solar farms to restore their power with a prespecified ramp rate so that any voltage and power oscillations can be prevented. No damping function is envisaged in these grid codes during the process of power ramp-up.

A novel power restoration technique is proposed in this paper, according to which the solar farm continues to perform POD during the entire power restoration process in the Partial PV-STATCOM mode. This prevents the recurrence of power oscillations while power is being restored to its pre-disturbance level. The proposed technique allows a much faster ramp rate to be achieved since power oscillations continue to be damped during the entire restoration process.

Two power restoration techniques are implemented in the PV Real Power Controllers shown in Fig. 6, and described below.

1) Power Restoration in a Ramped Manner

In this mode, the controller changes the PV real power output from zero to the pre-disturbance PV power level in a ramped manner with a ramp rate of K_{sl} starting at time $t = t_{st}$. This is the normal recommended mode for restoration of solar farms by grid codes [39] and smart inverter functions. No damping function is envisaged during ramp-up [17], [39].

2) Proposed Power Restoration in the Partial PV-STATCOM mode with POD control active

In this mode, the controller changes the PV real power output from zero to the pre-disturbance PV power level in a ramped manner with a ramp rate of K'_{sl} starting at time $t = t_{st}$. The solar farm is operated in the Partial PV-STATCOM mode with POD control active.

A variant of this technique is also shown in this paper, according to which the power is restored from zero to the pre-disturbance level in a nonlinear mode starting at $t = t_{st}$ with an exponential time constant t_c. This time constant can be determined based on the decay time constant of the ambient power oscillatory modes.

During real power restoration process, the solar farm performs POD in Partial PV-STATCOM mode with reactive power capacity available after real power generation at that time instant. The reactive power limit Q_{lim} which continuously keeps declining as the real power gets restored to its original pre-disturbance level is given by $Q_{lim} = \sqrt{S^2 - P^2}$, where, S represents the total inverter capacity, P is the inverter real power output and Q_{lim} is the maximum available inverter capacity during power restoration.

V. POD Optimized Controller Design

The POD controller parameters - *Gain*, *Lead* and *Lag* time constant are determined by the Simplex optimization technique [40] embedded in the PSCAD/EMTDC software [26]. In this paper, the aim is to minimize the low frequency power oscillations in line current. The corresponding Objective Function (OF) is defined as:

$$OF = \int_{T_1}^{T_2} \left(i_l - i_{l\_ref}\right)^2 dt \tag{3}$$

where, i_{l_ref} is the reference value of the midline current i_l. T_1 and T_2 are the start and end time instants of the current oscillations after the fault, respectively. The main concept of the embedded optimization is to run a *Slave* simulation to determine the value of the (OF) in the i_{th} run. The results are then sent to a *Master* project to check if the results are converging and a new set of POD controller parameters are generated for the $i+1^{th}$ iteration. The OF converges in about 40 and 59 runs for Study Systems 1 and 2, respectively.

VI. Small Signal Studies of Proposed POD control

The efficacy of the PV-STATCOM for POD at different locations is demonstrated through small signal residue analysis [29] in Matlab. The magnitude of residue is an indicator of the effectiveness of POD controller [29]. The higher the magnitude of the residue the better the location of PV-STATCOM for POD. In the Two-Area power system, five different locations considered for PV system placement are at buses 6, 7, 8, 9, and 10. Fig. 7 shows the residues for different PV-STATCOM locations with varying levels of power transfer from area *A* to *B* and vice versa. The highest residue for the maximum midline power transfer of 400 MW is observed at Bus 8 and hence the PV-STATCOM is connected to bus 8.

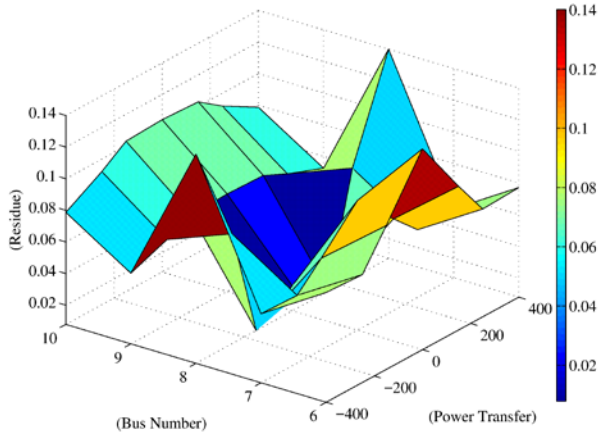

Fig. 7. Residue analysis for PV-STATCOM POD controller

VII. Case Study 1: The SMIB system

This case study presents the improvement in power transfer capability in Study System 1 (SMIB System) through power oscillation damping with the proposed PV-STATCOM control. A three phase to ground fault is initiated at generator bus at t = 2 sec for 5 cycles in the different studies. The simulations are performed using PSCAD/EMTDC software.

A. Power transfer without PV-STATCOM Control

Fig. 8 depicts the mid-line real power flow at the PCC bus

This article has been accepted for publication in a future issue of this journal, but has not been fully edited. Content may change prior to final publication. Citation information: DOI 10.1109/TSTE.2018.2871074, IEEE Transactions on Sustainable Energy

of the PV solar farm as well as the power output of the solar farm. In this study, as soon as the fault occurs, the PV solar farm is disconnected thereby reducing its power output from 100 MW to zero.

The line power transfer limit is evaluated by conducting a 5-cycle three-phase-to-ground fault for a given line power magnitude and observing the damping ratio of the ensuing power oscillations after the fault is cleared. The line power is gradually increased until the damping ratio of the power oscillations becomes just less than the utility acceptable value of 5% [1], [3], [41]. This magnitude of the power transfer is considered as the power transfer limit. Based on the above procedure, it is determined that the SMIB system can transfer at most 200 MW power from the synchronous generator in addition to the 100 MW power generated by the PV solar farm.

To examine the effect of increased power transfer, a similar fault study as above is conducted with 430 MW generator power. This results in unacceptably large power oscillations as shown in Fig. 8.

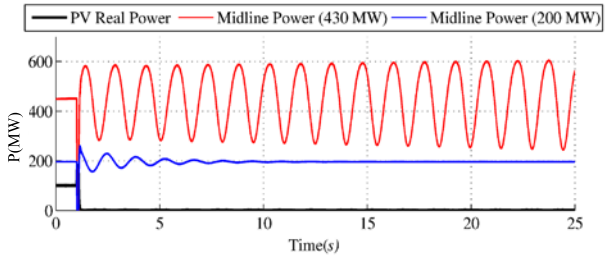

Fig. 8. Maximum power transfer capability of the SMIB system

B. *Power transfer with Full PV-STATCOM Damping Control and Power Restoration in Normal Ramped Manner*

This study is conducted with a generator power of 430 MW and PV solar farm producing its rated power output of 100 MW at mid-noon with maximum solar irradiance. Fig. 9 (a) depicts the midline power flow and the PV solar power output, whereas Fig. 9 (b) and (c) demonstrate the reactive power of the PV-STATCOM and PCC voltage, respectively. The proposed Full PV-STATCOM control utilizes the entire inverter capacity for reactive power modulation to successfully damp the power oscillations to within acceptable limits in 8 seconds. The PCC voltage is also rapidly stabilized.

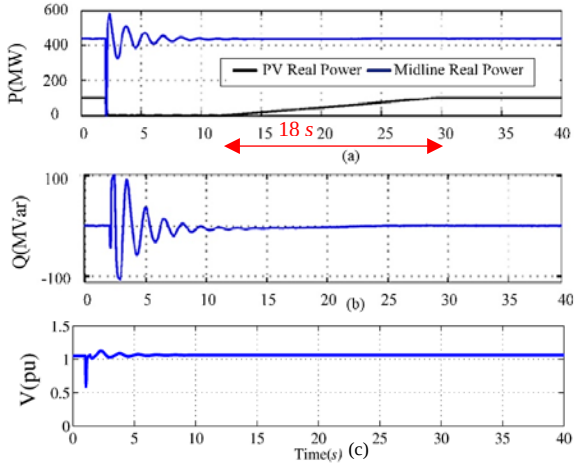

Fig. 9 (a) Midline and PV system real powers, (b) PV-STATCOM reactive power, (c) Midline voltage during POD and normal ramped power restoration.

It is recommended [18] that power restoration from a PV solar farm from zero to its rated level may be done with a typical ramp rate of 10% of rated capacity in 1 minute to avoid any power oscillations. In this case study, the fastest ramp rate which will expectedly not cause any resurrection of power oscillations is determined from simulations to be 5.5 MW/sec. Therefore, once power oscillations stabilize, the restoration of PV solar power output to its pre-disturbance value is commenced at t = 12 sec (incorporating the 2 sec factor of safety) with the above-obtained ramp rate of 5.5 MW/sec. It is noted that the power is completely restored in a period of 18 sec, with no ensuing power oscillations.

Power oscillation damping is accomplished by FACTS devices such as Static Var Compensators (SVCs) [1-3, 25, 29] and STATCOMs [4-7, 38] through dynamic reactive power control using their entire rated capacity. This helps increase the line power transfer capability which is limited from power oscillation damping considerations [1-3]. The proposed PV-STATCOM control transforms an existing PV solar farm into a STATCOM of same size. The PV-STATCOM therefore accomplishes an increase in power transfer capacity in a similar manner as an SVC or STATCOM. Although not included in this paper, system studies have shown that a smaller size PV solar farm (less than 100 MW) as PV-STATCOM causes a smaller increase in power transfer, whereas a larger size PV solar farm as PV-STATCOM results in a larger increase in power transfer. This performance is similar to SVCs and STATCOMs.

C. *Power transfer with Full PV-STATCOM Damping Control and Ramped Power Restoration with POD control active in Partial PV-STATCOM Mode*

This study is performed to demonstrate the effectiveness of the proposed restoration technique for the same system operating conditions as in previous Case B.

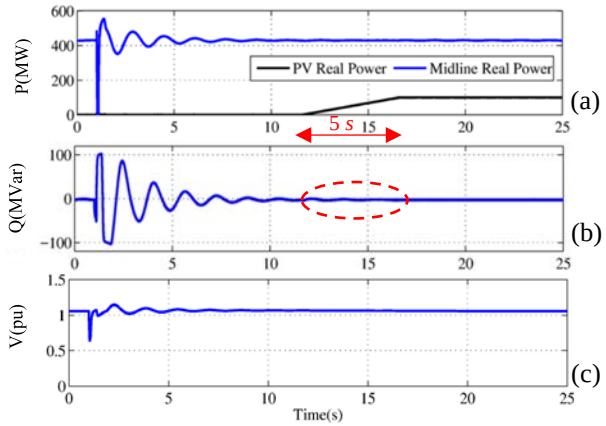

Fig. 10. (a) Midline and PV system real power, (b) PV-STATCOM reactive power, (c) Midline voltage during POD and power restoration in Partial PV-STATCOM damping mode.

Fig. 10 (a) depicts the midline power flow and the PV solar power output, whereas Fig. 10(b) and (c) illustrate the reactive power of the PV-STATCOM and PCC voltage, respectively. The PV real power is restored in a ramped manner with power oscillation damping continually being performed in the Partial PV-STATCOM mode during the ramp-up. For better illustration, the reactive power modulation during the restoration period is indicated in a red dashed circle. It is evident from Fig. 10 that with this novel restoration technique the

This article has been accepted for publication in a future issue of this journal, but has not been fully edited. Content may change prior to final publication. Citation information: DOI 10.1109/TSTE.2018.2871074, IEEE Transactions on Sustainable Energy

restoration of power to the pre-disturbance value is achieved in only 5 sec as compared to 18 sec in the previous case. This technique successfully prevents any recurrence of power or voltage oscillations.

D. *Nighttime Power transfer enhancement with Full PV-STATCOM Power Oscillation Damping Control*

The same 5 cycle fault at t = 2 sec is initiated for a generator power output of 430 MW at nighttime. Fig. 11 (a) portrays the behavior of 430 MW power flow in the tieline with and without the PV-STATCOM POD control. Fig. 11 (b) illustrates the reactive power of the PV-STATCOM. The solar farm with the proposed Full PV-STATCOM POD control successfully enables the same increase in power transfer from 200 MW to 430 MW in the nighttime, as in daytime.

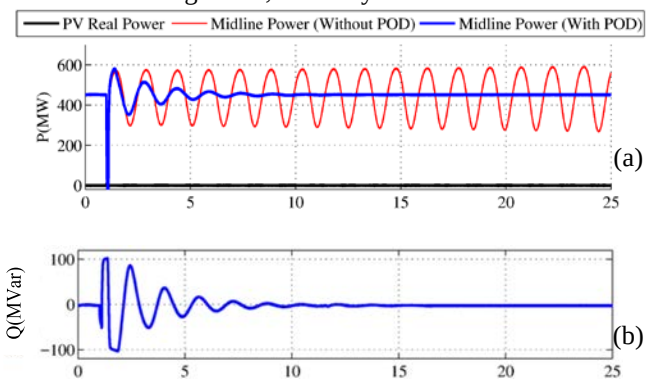

Fig. 11. Nighttime (a) Midline real power with and without POD with PV-STATCOM control, (b) PV-STATCOM reactive power during POD.

VIII. Case Study 2: Two-Area Power System

A. *Power transfer without PV-STATCOM Control*

In this case study for the two-area power system depicted in Fig. 3, the tie line power is transferred from Area *A* to Area *B* equally through Lines 1 and 2 under normal operation. A three phase to ground fault is initiated at t = 2 sec for 5 cycles in Line 2 close to Bus 9. The circuit breakers disconnect the faulted line 2 and the entire tie line power is subsequently transferred through Line 1. The midline connected PV solar farm is considered to produce its rated 100 MW power at noon under maximum solar irradiance.

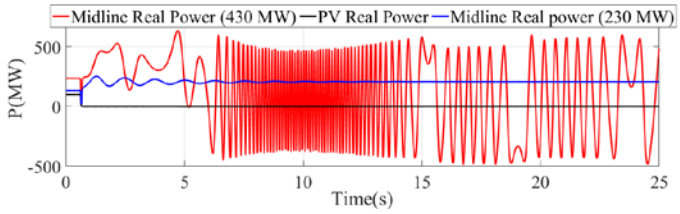

Fig. 12. Midline and PV real power in Two-Area system (230 MW and 430 MW power transfer)

Fig. 12 shows the midline real power and the PV solar power for this study. As soon as the fault occurs the PV solar farm is disconnected. Severe oscillations in power flow are observed if the prefault tie-line power is considered to be 430 MW. The maximum tie line power that can be stabilized post fault with a damping ratio of 5% [37] is 230 MW. In this study, the objective is to increase the line power transfer limit from 230 MW to 430 MW.

B. *Power transfer with Full PV-STATCOM Damping Control and Power Restoration in Normal Ramped Manner*

As soon as power oscillations are initiated, the solar power output is reduced to zero and the solar farm is transformed to Full PV-STATCOM with POD control. The proposed PV-STATCOM control then utilizes its entire inverter capacity for POD to stabilize the power system and increase the power transfer. Fig. 13 (a) illustrates the midline power and the PV real power. Figs. 13 (b) and (c) show the PV-STATCOM reactive power and PCC bus voltage, respectively. The PV-STATCOM POD function successfully stabilizes the power oscillations to within acceptable limits in about 10 sec (just before t = 12sec). The PCC voltage oscillations are also mitigated rapidly. The power restoration is commenced at t=15 sec, after a 2 sec delay for safety purpose. The solar power is ramped up to its pre-disturbance level of 100 MW at a rate of 5.5 MW/sec as determined earlier in about 18 sec.

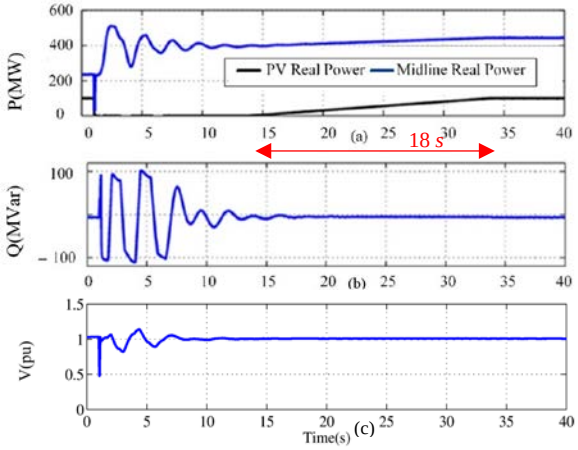

Fig. 13. (a) Midline and PV real power, (b) PV reactive power, (c) Midline voltage during POD and power restoration in a normal ramped manner.

C. *Power transfer with Full PV-STATCOM Damping Control and Ramped Power Restoration with POD control active in Partial PV-STATCOM Mode*

This study is performed to illustrate the efficacy of the proposed restoration technique for the same system operating conditions as in the previous Case B.

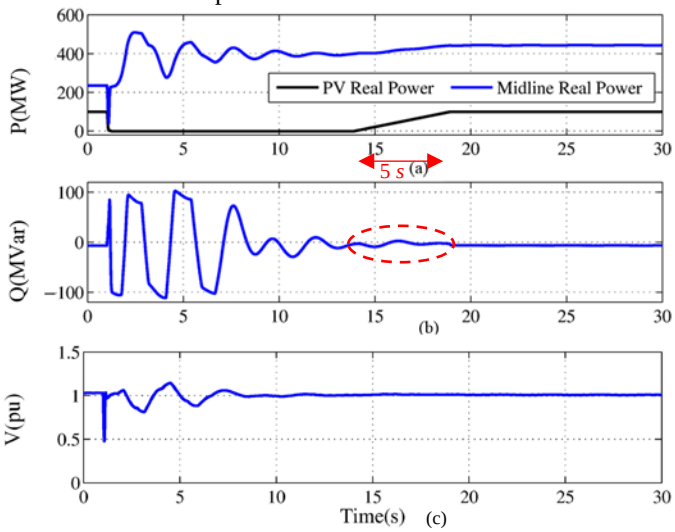

Fig. 14. (a) Midline and PV real power, (b) PV reactive power, (c) Midline voltage during POD and power restoration in a fast ramped manner.

This article has been accepted for publication in a future issue of this journal, but has not been fully edited. Content may change prior to final publication. Citation information: DOI 10.1109/TSTE.2018.2871074, IEEE Transactions on Sustainable Energy

Fig. 14 (a) depicts the midline power flow and the PV solar power output whereas Fig. 14 (b) and (c) demonstrate the reactive power of the PV-STATCOM and PCC voltage, respectively. It is evident that POD with Partial PV-STATCOM mode of operation reduces the time of PV power restoration to its pre-disturbance level of 100 MW in just 5 sec. This is 3.5 times faster than without the proposed restoration technique.

D. *Power transfer with Full PV-STATCOM Damping Control and Nonlinear Power Restoration with POD control active in Partial PV-STATCOM Mode*

This study is presented to show the effectiveness of an alternate technique of power restoration in a nonlinear (exponential) manner, after the power oscillations have been damped through POD control in Full PV-STATCOM mode of operation. The time constant of the exponential restoration is determined from a hit and trial process. During the restoration period, the POD function remains activated in Partial PV-STATCOM mode to damp the power oscillations. Fig. 15 illustrates the midline power flow and the PV solar power output for this case. In this case, 95% of entire pre-disturbance PV real power is restored within 2 *sec* and the remaining 5% is restored in 1 *sec*. The nonlinear PV restoration technique thus significantly reduces the restoration interval from 18 *s* to 3 *s*. This is presented just as an initial study. More work is needed to systematically determine the time constant of the exponential ramp-up, which is outside the scope of this paper.

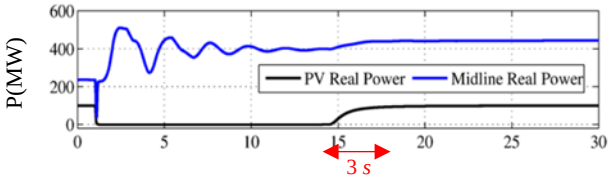

Fig. 15. Midline and PV real power when power is restored nonlinearly

E. *Nighttime Power transfer enhancement with Full PV-STATCOM Power Oscillation Damping Control*

The effectiveness of the proposed Full PV-STATCOM based POD control subsequent to the same fault as in Case A during nighttime is presented in this study.

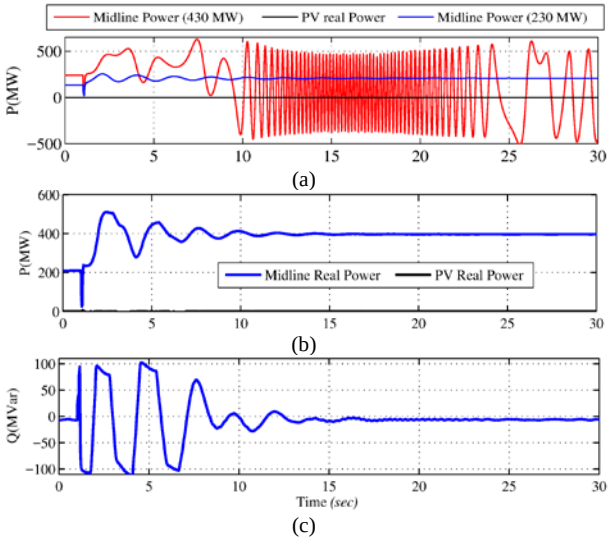

Fig. 16. Nighttime (a) Midline real power without POD with PV-STATCOM control, (b) Midline real power with Full PV-STATCOM POD Control, (c) PV-STATCOM reactive power.

Fig. 16 (a) portrays the behavior of 230 MW and 430 MW of power flow in the tieline without the PV-STATCOM control. Figs. 16(b) and (c) demonstrate the tieline power and PV system reactive power. The maximum power transfer in the tie line is only 230 MW. The proposed control increases the power transfer capability of the tieline from 230 MW to 430 MW, i.e., by 200 MW.

F. *Comparison between Partial and Full STATCOM*

The Partial STATCOM mode of PV-STATCOM is unable to provide any power oscillation damping during hours of full-sun. This is because the entire inverter capacity is used up for generating real power and no inverter capacity is left for POD through reactive power control. The Full-STATCOM mode of PV-STATCOM is therefore proposed in this paper based on patent [23], which allows the PV solar farm to provide POD with full inverter capacity even during hours of full sun.

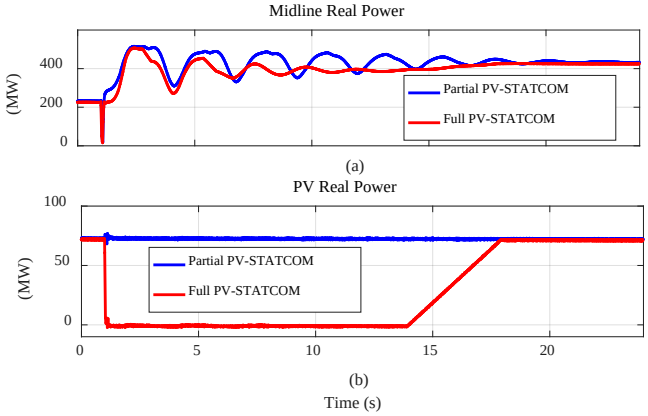

Fig. 17 a). Midline real power in Partial and Full STATCOM modes of operation; b) PV real power in Partial and Full STATCOM operating modes

A comparative study of Full and Partial STATCOM modes of operation of PV-STATCOM in Two-Area power system is presented for a PV power generation level of 80 MW (80% of its rated capacity). Fig. 17 depicts the mid line power and PV system real power when POD is performed with both Partial STATCOM operating mode (60 Mvar remnant inverter capacity) and Full STATCOM operating mode (100 Mvar full inverter capacity). If PV real power output is kept unchanged and POD is performed with Partial STATCOM operating mode, the oscillations in the midline real power get damped in 20 sec. However, if the real power output is reduced to zero and POD is performed with Full STATCOM operating mode, the midline real power oscillations are damped within 10 sec. This study clearly demonstrates the effectiveness of the Full STATCOM mode of operation over the Partial STATCOM operating mode.

IX. Effect of PV-STATCOM Control on System Frequency and PV System Losses

The proposed POD utilizing reactive power control is not expected to create any adverse impact on system frequency. The proposed PV-STATCOM control provides only damping of power oscillations. This may indirectly alleviate the frequency deviations as well. Fig. 18 depicts the power system frequency with POD control with PV-STATCOM (Case C) and without POD control (Case A) of the Two-Area power system

This article has been accepted for publication in a future issue of this journal, but has not been fully edited. Content may change prior to final publication. Citation information: DOI 10.1109/TSTE.2018.2871074, IEEE Transactions on Sustainable Energy

considering a tie-line power flow of 430 MW. For the two-area study system, it is shown from Fig. 18 that that the proposed POD control of PV-STATCOM not only damps power oscillations but also reduces the frequency oscillations that would be caused in the absence of such a control.

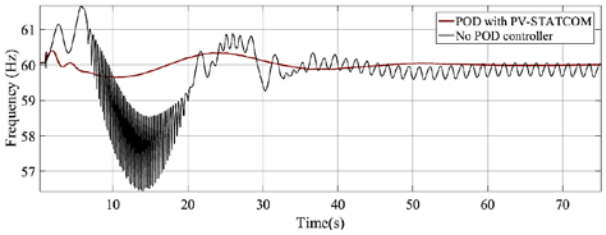

Fig. 18. Effect of PV-STATCOM control on system frequency in Two-Area Power System

The proposed PV-STATCOM control transforms an existing large PV solar into a STATCOM of same size (rating). The losses in PV-STATCOM during POD will be similar to the losses in an actual STATCOM of equivalent size, which are acceptable in power industry.

X. Case Study 3: 12 Bus FACTS Power System

This section presents the efficacy of the proposed PV-STATCOM POD control on the more complex modified 12 bus FACTS power system [30, 31]. According to [31], a permanent disconnection of line between bus 4 and 5 following a fault causes low frequency oscillations to appear in Generator 3 and 4. These oscillation can be damped individually with 100 Mvar SVC unit at bus 4 [31]. In this section the same functionality of SVC in [31] is achieved with the proposed POD controller of PV-STATCOM in Full STATCOM mode. To damp both G_3 and G_4 oscillations, ω_3 and ω_4 are used as control signals for the POD controllers. Fig. 19 illustrates the result for POD with PV-STATCOM in the 12 bus FACTS power system. At t =5 sec, the line between bus 4 and 5 is disconnected after a three-phase fault at bus 4 for 5 cycles.

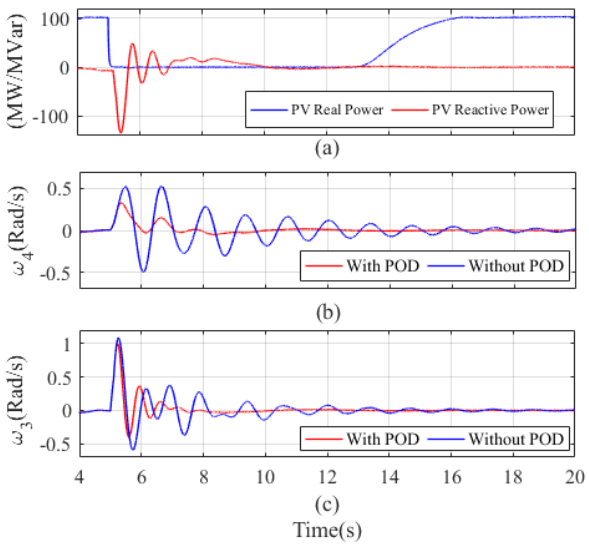

Fig. 19. (a) PV-STATCOM real and reactive power, (b) Generator 4 speed deviation (c) Generator 3 speed deviation in 12 bus FACTS power system.

Fig. 19(a) illustrates that as soon as low frequency electromechanical oscillations appear, the PV system operation switches from the conventional mode to PV-STATCOM mode and damps the oscillations. Once the oscillations decay to less than the acceptable limit, the PV real power is restored to the prefault level of P_{pr}=100 MW with the proposed restoration technique described in Section VIII D. Fig. 19 (b) and Fig. 19(c) depict the speed deviations of generators G_4, and G_3 respectively. It is clearly seen that the proposed PV-STATCOM controller successfully damps the power oscillations in 3 *sec*. Furthermore, the PV real power restoration has no adverse effect on the speeds of the generators.

XI. Conclusion

This paper presents a novel smart control of transmission line connected large PV solar system as a STATCOM, termed PV-STATCOM, for damping power oscillations and thereby substantially increasing the power transfer capacity of the network. The proposed control provides POD through reactive power modulation utilizing the entire inverter capacity during nighttime. During daytime the solar farm discontinues its real power generation function very briefly (about 15 sec) and utilizes its entire inverter capacity for POD. It subsequently restores power generation to its pre-disturbance level in a gradual manner while keeping the POD function activated utilizing the remaining inverter capacity. EMTDC/PSCAD simulation studies demonstrate the effectiveness of the proposed PV-STATCOM control in a single machine infinite bus (SMIB) system which exhibits local inertial oscillatory mode, two-area system which displays both local inertial and inter-area modes of oscillations, and the 12 bus FACTS power system which has multiple interarea modes of oscillations.

In SMIB system, a 100 MW midline connected PV solar system increases the power transfer capacity by 230 MW, whereas in the Two-Area system a 100 MW PV solar system increases the power transmission limit by 200 MW. Moreover, the proposed power restoration technique keeping POD activated is more than 3 times faster than that specified by grid codes (without POD function). The temporary (about 18 sec) shutdown of real power production function for POD is not seen to cause any adverse impact on system frequency.

The proposed PV-STATCOM provides 24/7 functionality of an equivalent STATCOM for POD at the same location. This PV-STATCOM is expected to be about 50-100 times lower in cost than an equivalent STATCOM as it utilizes the existing infrastructure (substation, bus-work, transformers, circuit breakers, protection systems, etc.) of a PV solar farm to transform it into a full scale STATCOM of similar size.

The PV-STATCOM as an alternate FACTS device is expected to bring significant savings for utilities seeking to increase their power transmission capacity. It also opens a new revenue making opportunity for transmission connected solar farms to provide 24/7 STATCOM functionality at substantially lower cost. Implementation of this technology of course requires appropriate agreements among utilities, system regulators, solar farm developers and inverter manufacturers.

The objective of this paper is to propose a novel control of a single PV solar farm as PV-STATCOM for power oscillation damping during day and night. If the PV-STATCOM control is implemented on multiple PV solar farms in electrical proximity,

the PV-STATCOM controls will need to be coordinated in a similar manner as coordination of multiple FACTS devices, and HVDC and FACTS devices [3,38, 41, 44-47]. The control coordination among multiple PV-STATCOMs will ensure that all the participating PV-STATCOMs will simultaneously provide power oscillation damping and concurrently return to normal operation after the oscillations are damped out. This control coordination requires detailed control design and system studies, which are outside the scope of the present paper.

XII. References

[1] P. Kundur, N. J. Balu, and M. G. Lauby, Power system stability and control vol. 7: McGraw-hill New York, 1994.

[2] N. G. Hingorani and L. Gyugyi, Understanding FACTS: concepts and technology of flexible AC transmission systems: Wiley-IEEE press, 2000.

[3] R. M. Mathur and R. K. Varma, Thyristor-based FACTS controllers for electrical transmission systems: John Wiley & Sons, 2002.

[4] Y. Xiao, Y. Song, C.-C. Liu, and Y. Sun, "Available transfer capability enhancement using FACTS devices," IEEE Trans. Power systems, vol. 18, pp. 305-312, 2003.

[5] X. Y. Bian, Y. Geng, K. L. Lo, Y. Fu, and Q. B. Zhou, "Coordination of PSSs and SVC Damping Controller to Improve Probabilistic Small-Signal Stability of Power System With Wind Farm Integration," IEEE Trans. Power Systems, vol. 31, pp. 2371-2382, 2016.

[6] M. Haque, "Improvement of first swing stability limit by utilizing full benefit of shunt FACTS devices," IEEE Trans. Power Systems, pp. 1894-1902, 2004.

[7] N. Mithulananthan, C. A. Canizares, J. Reeve, and G. J. Rogers, "Comparison of PSS, SVC, and STATCOM controllers for damping power system oscillations," IEEE Trans. Power Systems, pp. 786-792, 2003.

[8] A. M. Simões, D. C. Savelli, P. C. Pellanda, N. Martins, and P. Apkarian, "Robust design of a TCSC oscillation damping controller in a weak 500-kV interconnection considering multiple power flow scenarios and external disturbances," IEEE Trans. power systems, vol. 24, pp. 226-236, 2009.

[9] S. Arabi, H. Hamadanizadeh, and B. B. Fardanesh, "Convertible static compensator performance studies on the NY state transmission system," IEEE Trans. Power Systems, vol. 17, pp. 701-706, 2002.

[10] The World's Largest Solar Plant Is Now Online in India. Available: http://www.popularmechanics.com/science/green-tech/a24063/worlds-largest-solar-plant-india/

[11] C. Tiba and E. d. A. Ricardo, "Siting PV plant focusing on the effect of local climate variables on electric energy production–Case study for Araripina and Recife," Renewable Energy, vol. 48, pp. 309-317, 2012.

[12] Fact Sheet California Valley Solar Ranch. Available: https://us.sunpower.com/sites/sunpower/files/media-library/fact-sheets/fs-california-valley-solar-ranch-factsheet.pdf

[13] A. Sharma, "A comprehensive study of solar power in India and World," Renewable and Sustainable Energy Reviews, vol. 15, pp. 1767-1776, 2011.

[14] R. Shah, N. Mithulananthan, R. Bansal, and V. Ramachandaramurthy, "A review of key power system stability challenges for large-scale PV integration," Renewable and Sustainable Energy Reviews, vol. 41, pp. 1423-1436, 2015.

[15] S. Eftekharnejad, V. Vittal, G. T. Heydt, B. Keel, and J. Loehr, "Small Signal Stability Assessment of Power Systems With Increased Penetration of Photovoltaic Generation: A Case Study," IEEE Trans. Sustainable Energy, vol. 4, pp. 960-967, 2013.

[16] B. Tamimi, C. Cañizares, and K. Bhattacharya, "System stability impact of large-scale and distributed solar photovoltaic generation: the case of Ontario, Canada," IEEE Trans. Sust. Energy, vol. 4, pp. 680-688, 2013.

[17] B. Seal, "Common functions for smart inverters, version 3," ed: EPRI Report 3002002233, Palo Alto, CA, 2013.

[18] M. Morjaria, D. Anichkov, V. Chadliev, and S. Soni, "A Grid-Friendly Plant: The Role of Utility-Scale Photovoltaic Plants in Grid Stability and Reliability," IEEE Power and Energy Magazine, vol. 12, pp. 87-95, 2014.

[19] R. K. Varma, V. Khadkikar, and R. Seethapathy, "Nighttime Application of PV Solar Farm as STATCOM to Regulate Grid Voltage," IEEE Trans. Energy Conversion, vol. 24, pp. 983-985, 2009.

[20] R. K. Varma, S. A. Rahman, and T. Vanderheide, "New Control of PV Solar Farm as STATCOM (PV-STATCOM) for Increasing Grid Power Transmission Limits During Night and Day," IEEE Trans. Power Delivery, vol. 30, pp. 755-763, 2015.

[21] R. Shah, N. Mithulananthan, and K. Y. Lee, "Large-scale PV plant with a robust controller considering power oscillation damping," IEEE Trans. Energy Conversion, vol. 28, pp. 106-116, 2013.

[22] R. G. Wandhare and V. Agarwal, "Novel Stability Enhancing Control Strategy for Centralized PV-Grid Systems for Smart Grid Applications," IEEE Trans. Smart Grid, vol. 5, pp. 1389-1396, 2014.

[23] Rajiv K. Varma, "Multivariable Modulator Controller for Power Generation Facility", PCT Application (PCT/CA2014/051174) filed on December 6, 2014

[24] V. Gevorgian and S. Booth, "Review of PREPA technical requirements for interconnecting wind and solar generation," National Renewable Energy Lab.(NREL), Golden, CO (United States) 2013.

[25] K. R. Padiyar and R. K. Varma, "Damping torque analysis of static VAR system controllers," IEEE Trans. Power Systems, vol. 6, pp. 458-465, 1991.

[26] A. M. Gole, S. Filizadeh, R. W. Menzies, and P. L. Wilson, "Optimization-enabled electromagnetic transient simulation," IEEE Trans Power Delivery, vol. 20, pp. 512-518, 2005.

[27] B. K. Kumar, S. N. Singh, and S. C. Srivastava, "Placement of FACTS controllers using modal controllability indices to damp out power system oscillations," IET Gen., Trans. & Dist., vol. 1, pp. 209-217, 2007.

[28] M. M. Farsangi, H. Nezamabadi-pour, Y. H. Song, and K. Y. Lee, "Placement of SVCs and Selection of Stabilizing Signals in Power Systems," IEEE Trans. Power Systems, vol. 22, pp. 1061-1071, 2007.

[29] N. Martins and L. T. Lima, "Determination of suitable locations for power system stabilizers and static var compensators for damping electromechanical oscillations in large scale power systems," IEEE Trans. Power Systems, vol. 5, pp. 1455-1469, 1990.

[30] S. Jiang, U. D. Annakkage, and A. M. Gole, "A platform for validation of FACTS models," IEEE Trans. Power Del., pp. 484–491, Jan. 2006.

[31] G. K. Venayagamoorthy and S. R. Jetti, "Dual-function neuron-based external controller for a static var compensator," *IEEE Trans. Power Delivery*, vol. 23, pp. 997-1006, 2008.

[32] S. A. Rahman, R. K. Varma, and T. Vanderheide, "Generalised model of a photovoltaic panel," IET Renewable Power Generation, vol. 8, pp. 217-229, 2014.

[33] A. Yazdani and R. Iravani, Voltage-sourced converters in power systems: modeling, control, and applications: John Wiley & Sons, 2010.

[34] A. Reznik, M. G. Simoes, A. Al-Durra, and S. Muyeen, "LCL filter design and performance analysis for grid-interconnected systems," IEEE Trans. Industry Applications, vol. 50, pp. 1225-1232, 2014.

[35] A. Yazdani, A. R. Di Fazio, H. Ghoddami, M. Russo, M. Kazerani, J. Jatskevich, et al., "Modeling guidelines and a benchmark for power system simulation studies of three-phase single-stage photovoltaic systems," IEEE Trans. Power Delivery, vol. 26, pp. 1247-1264, 2011.

[36] A. Yazdani and R. Iravani, "A neutral-point clamped converter system for direct-drive variable-speed wind power unit," IEEE Trans. energy conversion, vol. 21, pp. 596-607, 2006.

[37] A. Yazdani and P. P. Dash, "A Control Methodology and Characterization of Dynamics for a Photovoltaic (PV) System Interfaced With a Distribution Network," IEEE Trans. Power Delivery, vol. 24, pp. 1538-1551, 2009.

[38] Y. Li, C. Rehtanz, S. Ruberg, L. Luo, and Y. Cao, "Wide-Area Robust Coordination Approach of HVDC and FACTS Controllers for Damping Multiple Interarea Oscillations," IEEE Trans. Pwr Del., p1096-1105, 2012.

[39] "Generating plants connected to the medium-voltage network," Technical Guideline of BDEW, 2008.

[40] J. A. Nelder and R. Mead, "A simplex method for function minimization," The computer journal, vol. 7, pp. 308-313, 1965.

[41] "Impact of Interactions Among Power System Controls," CIGRE Technical Brochure No. 166, Paris, August 2000.

[42] "Reliability Standards for the Bulk Electric Systems of North America", North American Electric Reliability Corporation, 2017.

[43] ERCOT Nodal Operating Guides", Electric Reliability Council of Texas, 2015, Available: http://www.ercot.com/mktrules/guides/noperating/cur

[44] "Coordination of Controls of Multiple FACTS/HVDC Links in the Same System," CIGRE Technical Brochure No. 149, Paris, December 1999.

[45] "Analysis of Control Interactions on FACTS Assisted Power Systems," EPRI Report TR-109969 Palo Alto, CA, January 1998.

[46] L. Gerin-Lajoie, G. Scott, S. Breault, E. V. Larsen, D. H. Baker, and A. F. Imece, "Hydro-Quebec Multiple SVC Application Control Stability Study," IEEE Trans. Power Delivery, July 1990, pp. 1543–1551.

[47] J. J. Sanchez-Gasca, "Coordinated Control of Two FACTS Devices for Damping Inter-Area Oscillations," IEEE Trans.Power Sys., Vol. 13, No. 2, May 1998, pp. 428–434.

This article has been accepted for publication in a future issue of this journal, but has not been fully edited. Content may change prior to final publication. Citation information: DOI 10.1109/TSTE.2018.2871074, IEEE Transactions on Sustainable Energy

XIII. BIOGRAPHY

Rajiv K. Varma (M'90-SM'09) obtained B.Tech. and Ph.D. degrees in Electrical Engineering from Indian Institute of Technology (IIT), Kanpur, India, in 1980 and 1988, respectively. He is currently a Professor with The University of Western Ontario (UWO), London, ON, Canada. He was the Hydro One Chair in power systems engineering with UWO from 2012 to 2015. Prior to this position, he was a faculty member in the Electrical Engineering Department at IIT Kanpur, India, from 1989-2001. He has co-authored an IEEE Press/Wiley book on Thyristor Based FACTS Controllers. He has co-delivered several Tutorials (IEEE sponsored), Courses and Workshops on Smart Inverters, FACTS, SVC and HVDC in different countries. His research interests include FACTS, power systems stability, and grid integration of photovoltaic solar and wind power systems. He is presently the Vice Chair of the IEEE "HVDC and FACTS Subcommittee" and Chair of IEEE Working Group 15.05.17 on "HVDC and FACTS Bibliography" since 2004.

Hesamaldin Maleki received his Bachelor's degree in Electrical Engineering from Chamran University of Ahvaz, Iran in 2010. He obtained his M.Sc. degree in Electrical Engineering, Power Systems from Universiti Tenaga Nasional (UNITEN), Kajang, Malaysia, in 2013. During his Master's degree, he was also working as a research assistant in Power Quality Research Group Center at UNITEN university. He subsequently received his Ph.D degree in Electrical and Computer Engineering from The University of Western Ontario (UWO), London, ON, Canada, in 2017. During his Ph.D studies, he was Teaching Assistant for several courses at UWO. He is currently working at Hatch Ltd as an Electrical System Designer. His research interests include FACTS, SVC, HVDC, Battery Energy Storage Systems (BESS), power system stability, power system small signal and transient analysis.